RESEARCH ARTICLE

• Arch Hyg Sci 2019;8(1):35-45
• Journal Homepage: http://jhygiene.muq.ac.ir

Degradation of Acid Orange 7 Dye with PMS and H_2O_2 Activated by $CoFe_2O_4$/PAC Nanocomposite

Shirin Esmaeili[a], Mahboobeh Dehvari[b], Ali Akbar Babaei[c*]

[a]Department of Environmental Health Engineering, School of Health, Ahvaz Joundishapour University of Medical Sciences, Ahvaz, Iran.
[b]Student Research Committee, Department of Environmental Health Engineering, School of Health, Ahvaz Joundishapour University of Medical Sciences, Ahvaz, Iran.
[c]Environmental Technologies Research Center, Department of Environmental Health Engineering, School of Health, Ahvaz Joundishapour University of Medical Sciences, Ahvaz, Iran.

***Correspondence** should be addressed to Dr Ali Akbar Babaei, **Email:** ababaei52@gmail.com

A-R-T-I-C-L-EI-N-F-O

Article Notes:
Received: Sep 13, 2018
Received in revised form: Feb 24, 2019
Accepted: Feb 28, 2019
Available Online: Marc 14, 2019

Keywords:
Acid Orange 7,
Nanocomposite,
Peroxymonosulfate,
Hydrogen Peroxide,
Iran.

A-B-S-T-R-A-C-T

Background & Aims of the Study: Discharge of untreated colored wastewater into aquatic environments could cause problems such as cancer. Among the various treatment methods, advanced oxidation processes (AOPs) have attracted much attention in recent years. The aim of this study was the removal of acid orange 7 dye using $CoFe_2O_4$@PAC nanocomposite in the presence of peroxymonosulfate (PMS) and hydrogen peroxide (H_2O_2).
Materials & Methods: The various variables effect including pH, catalyst dose, peroxymonosulfate and hydrogen peroxide concentration, reaction time, and initial dye concentration were evaluated. The synthesized nanocomposite was characterized by SEM, EDX, XRD and BET analyses. The residual concentration of AO7 dye was determined using UV–Vis spectrophotometer at wavelength of 485 nm.
Results: It was found that decolorization increases by increasing the catalyst dosage and reaction time, and decreasing pH. With increasing the dye initial concentration from 10 mg/L to 250 mg/L, in the presence of H_2O_2 and PMS dye removal decreased from 99.5% to 39.7% and from 99.9% to 43.7%, respectively. The adsorption kinetics was found to follow pseudo-first-order kinetic model (R^2>0.99).
Conclusions: The results indicated that the prepared composite could be used as an effective and environmental friendly magnetic adsorbent for the removal of AO7 dye from aqueous solutions.

Please cite this article as: Esmaeili S, Dehvari M, Babaei A A. Degradation of Acid Orange 7 Dye with PMS and H_2O_2 Activated by $CoFe_2O_4$/PAC Nanocomposite. Arch Hyg Sci 2019;8(1):35-45

Background

Every day, many harmful organic pollutants such as dyes are discharged into the environment by industries (1). Azo dyes are carcinogenic and mutagenic compounds and constitute the largest class of dyes. Colored wastewater discharged into receiving waters leads to environmental contamination such as reduced sunlight penetration and toxicity to the aquatic life (2,3). The orange acid 7 (AO7) is an acidic dye, soluble in water and has an azo group. Because azo dyes are not easily degraded, they must be removed prior to discharged into the water (4,5). So far, different methods have been used to remove these pollutants from industrial wastewater. Today, advanced oxidation processes (AOPs) based on nanoparticles, due to high efficiency and no secondary contamination, to remove a variety of contaminants such as dyes have been used (6). AOPs are based on generation of reactive radical species such as sulfate, superoxide or hydroxyl. Hydroxyl radicals ($OH^{\cdot}$) with high oxidizing and non-

selective oxidizing properties are the key oxidizing agent of advanced oxidation processes (7). Sulfate radical-based AOPs are considered as one of the most advanced oxidation processes due to their high oxidizing properties and are seriously considered for the removal of resistant and biodegradable organic pollutants (8,9). Besides the high oxidation–reduction potential (2.6 V), sulfate radicals can also be attractive for application in chemical oxidation due to their high solubility in water, high stability and relative low cost (10,11).

Proxymonosulfate (HSO5-, PMS) is a non-selective anion, soluble and the strongest oxidant in the Peroxygen family. It has unique properties including higher standard reduction potential than hydroxyl radicals and less dependence on natural materials. Under atmospheric conditions, the oxidation of proxymonosulphate does not have much effect on organic pollutants. The activation of PMS can be done by heat, light, or certain metal ions (Fe_2^+, Co_2^+,…) (12). According to previous studies, hydrogen peroxide (H_2O_2) is an oxidizing agent that acts as a source for reactive oxygen species and can lead to oxidizing of various organic pollutants. H_2O_2 decomposes slowly at room temperature, so H_2O_2 activation is necessary to produce oxidizing hydroxyl radicals (13-15).

So far, the effectiveness of various adsorbents including active carbon, bentonite, lignin, quartz, kaolinite and other adsorbents has been evaluated as a catalyst bed for the removal of pollutants (7). Powdered activated carbon (PAC) as the most common and most effective adsorbent is known for effective removal of dyes due to high absorption capacity, high surface area and low cost (16). The main problem in the use of nanocomposites or nanoparticles is their separation from the solution due to their small size. The separation of nanocomposite carbon from aqueous solutions using methods such as filtration and centrifugation is difficult, time-consuming and costly. Therefore, the dispersion, and production of secondary pollution are the main problems of these systems (17). Magnetic separation is a method to facilitate the separation of these nanocomposites (18).

Magnetic nanoparticles coated on activated carbon were used for the removal of different pollutants (19,20). Among the magnetic nanoparticles, spherical ferrite structures (AFe_2O_4; A is a divalent metal cation such as Fe, Cu, Ni, Co, Mg, Mn) has been paid much attention to synthesize magnetic nanocomposites in order to improve the catalyst regeneration (21,22). Cobalt ferrite ($CoFe_2O_4$) nanoparticles had properties such as excellent chemical stability, rapid separation and moderate saturation magnetization (18,22-23).

The catalyst used in this study is iron oxide and cobalt nanoparticles ($CoFe_2O_4$) stabilized on powdered activated carbon that in the presence of peroxymonosulfate and hydrogen peroxide, it can produce sulfate and possibly hydroxyl radicals, and thus can lead to the degradation and removal of organic compounds from the wastewater sample.

Aims of the study:

The aim of this study is the investigation of $CoFe_2O_4$@PAC nanocomposite efficiency in the presence of peroxymonosulfate (PMS) and hydrogen peroxide (H_2O_2) for the removal of acid orange 7 dye from aqueous solutions.

Materials & Methods

Materials

The acid orange 7 (AO7) was purchased from Alvan Sabet company, Iran. The characteristics of AO7 dye is shown in Table 1 (24, 25). All the other reagents were of analytical grade that were used without further purification. $FeCl_2.4H_2O$, $FeCl_3.6H_2O$, $Co(NO_3)_2.6H_2O$, ammonia hydroxide, and nitric acid were purchased from Merck and used to synthesis the $CoFe_2O_4$@PAC nanocomposite.

Table 1) Characterization of Acid Orange 7 dye

Chemical structure	Molecular formula	Molar mass	λ_{max}

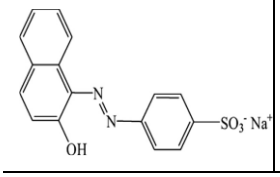	$C_{16}H_{11}N_2NaO_4S$	350.32 (g/mol)	485 (nm)

Synthesis of nanocomposite

The catalyst used in this study ($CoFe_2O_4$) that was supported on the modified powdered activated carbon (PAC), was synthesized by co-precipitation method. First, certain amount of activated carbon powder (98% purity, Merck) was dissolved in nitric acid 65%. Then, the solution was stirred at 80 ˚C for 3 hours. The sample was washed by ultrapure water and then was dried in an oven at 80 ˚C overnight.

5.652 g $FeCl_2.4H_2O$, 3.841 g $FeCl_3.6H_2O$ and 4.133 g $Co(NO_3)_2.6H_2O$ (Fe(III):Fe(II):Co(II)=1:2:1) were added to 80 mL of ultrapure water. 5 g modified activated carbon powder (prepared in the previous step) was added to the solution. With stirring, the solution was mixed for 0.5 h with nitrogen bubbling at 90 ˚C. Then, 40 mL ammonia hydroxide (28%) was added drop wisely at 30 min to make solution pH 10-11. Nitrogen gas flow stopped and to ensure the completion of the reaction, the mixture was stirred for one hour. The sample was then washed by ethanol and ultrapure water for several times (pH=7). Then was dried at 100 ˚C for 8h. It was calcinated in the furnace without oxygen (Nabertherm High-Temperature Tube Furnace) at temperature rate of 5 ˚C/min at 500 ˚C for 4 h (26). Finally, the black solid was formed ($CoFe_2O_4$@PAC, Figure 1). For the use in advanced oxidation process, it was stored inside the desiccator. As shown in the inset of Figure 2d, the magnetic separation performance of the composite was tested by placing a magnet (~4000 Gauss) near the glass bottle. The product was attracted toward the magnet in a short period, demonstrating its high magnetic sensitivity. These results indicate that the composite can be potentially used as a magnetic adsorbent to remove dye contaminants from aqueous solution in order to avoid the secondary pollution.

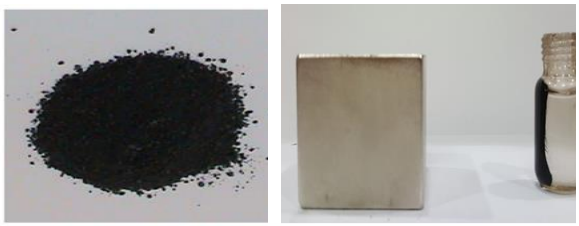

Figure 1) The synthesized catalyst and its magnetic behavior in the vicinity of a strong magnet

Characterization of nanocomposite

To study the surface morphologies of nanocomposite, scanning electron microscopy (SEM) was done. In order to the crystal structural characterization of nanoparticles, X-ray diffraction analysis (XRD) was performed by X-ray diffractometer. Energy dispersive X-ray spectroscopy (EDS) analysis, using an EDX chemical microanalysis module, was used to determine the elemental composition of the samples. The BET (Brunauer–Emmett–Teller) surface area was determined by Micromeritics analyzer under liquid nitrogen environment.

Experiments procedure

Stock solution was prepared by dissolving a known quantity of the dye in distilled water; this solution was diluted to the required initial concentrations (10-250 mg/l). In each stage, the certain amount of nanocomposite added to 50 mL of AO7 solution in a 100 ml Erlenmeyer flask. Then, H_2O_2 and PMS in certain values were added. The pH of the suspension was adjusted by 0.1 M HCl or NaOH solutions. Batch experiments were carried out using an orbital shaker at 250 rpm. At different time intervals, the solution was sampled and a powerful magnet was used for the magnetic separation of the absorbent from the solution. The residual AO7 dye solution concentration was determined using UV–Vis spectrophotometer at wavelength of 485 nm (25). The dye removal efficiency (%R) using nanocomposite was calculated using equation (1):

$$R(\%) = \frac{(C_0 - C_t)}{C_0} \times 100 \qquad (1)$$

C_t and C_o are the equilibrium and initial dye concentrations (mg/L), respectively (3).

The effect of the various parameters, contact time (0–120 min), initial dye concentration (10-250 mg/L), catalyst dosage (0.1-1.5 g/L), solution pH (3-11), PMS concentration (2.5-50 µM) and H_2O_2 concentration (1-15 mM) were investigated. All experiments were repeated three times.

Data analysis:

Data analysis has been done using Excel software.

Results

The characterization of nanocomposite

Figure 2a shows the SEM image of the $CoFe_2O_4$@PAC composite. It can be seen that nanocomposite is spherical (sphere shaped). The approximate crystallite size of nanoparticles (D) was calculated using Scherer's equation (Eq. 2).

$$D = \frac{0.9\lambda}{\beta \cos\theta} \qquad (2)$$

Where, λ is the X-ray wavelength (1.540598 Å), β is the full-width at half-maximum, and Θ is the diffraction angle (27). The approximate crystallite size of $CoFe_2O_4$@PAC was found in the range of 33.97-39.60 nm.

The XRD patterns of $CoFe_2O_4$@PAC, $CoFe_2O_4$ and PAC are presented in Figure 2b. The XRD patterns show the sharp peaks at 2θ values of 19.98, 30, 36.95, 38.21, 43.25, 56.65, 58.30, and 62 that correspond to 111, 220, 311, 222, 400, 422, 511 and 440 planes. Also the XRD pattern indicated that the $CoFe_2O_4$@PAC structure obtained by the process is crystalline. The XRD pattern in Figure 2b shows a peak at around 26◦ that correspond to the graphite (002) plane of the PAC (18).

Figure 2c shows energy dispersive X-ray spectroscopy (EDX) analysis. The EDX spectra confirmed the presence of Fe, Co, Ca, Cl, C, and O elements.

Physical and structural properties of Co-Fe_2O_4@PAC nanocomposite is presented in Table 2. The BET surface area of Co-Fe_2O_4@PAC was 595.6 m^2/g. The pore volume of Co-Fe_2O_4@PAC nanocomposite was 0.316 cm^3/g due to the presence of carbon that leads to the surface roughness (18).

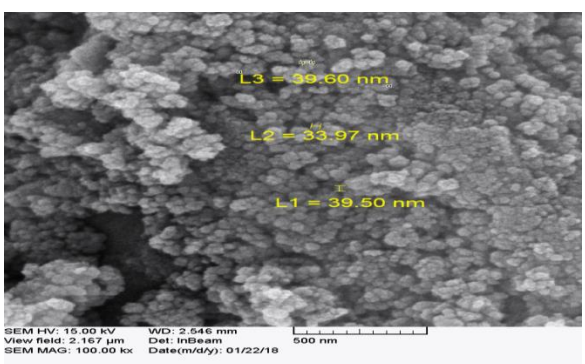

(a)

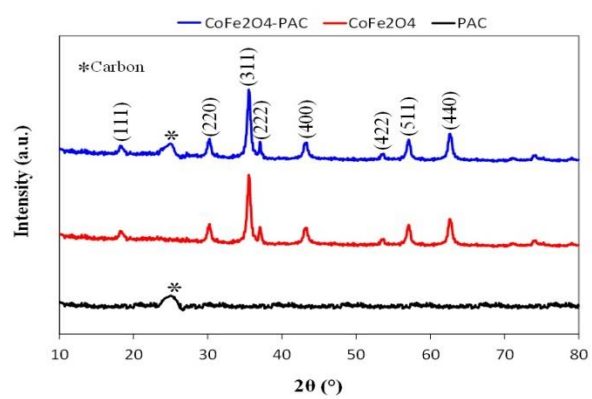

(b)

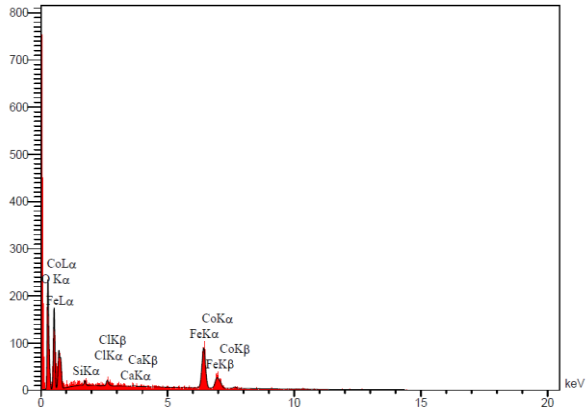

Elt	Line	Int	Error	K	Kr	W%	A%	ZAF	Formula	Ox%	Cat#
C	Ka	49.8	9.2016	0.3983	0.1960	45.52	63.30	0.4305		0.00	0.00
O	Ka	39.5	9.2016	0.1573	0.0774	27.30	28.50	0.2835		0.00	0.00
Si	Ka	2.4	0.6151	0.0035	0.0017	0.23	0.14	0.7385		0.00	0.00
Cl	Ka	4.0	0.6253	0.0083	0.0041	0.48	0.23	0.8449		0.00	0.00
Ca	Ka	0.8	0.2743	0.0021	0.0010	0.11	0.05	0.9162		0.00	0.00
Fe	Ka	48.2	0.7602	0.3340	0.1643	20.31	6.07	0.8090		0.00	0.00
Co	Ka	11.3	0.7602	0.0965	0.0475	6.05	1.71	0.7853		0.00	0.00
				1.0000	0.4919	100.00	100.00			0.00	0.00

(c)

Figure 2) Characterization of Co-Fe_2O_4@PAC nanocomposite

a) SEM image; b) XRD spectra pattern; c) EDX spectrum

Table 2) Physical and structural properties of Co-Fe_2O_4@PAC nanocamposite compared to Co-Fe_2O_4 and PAC

Sample	Color	Pore structure	Pore diameter (nm)	Pore volume (cm^3/g)	Specific surface (m^2/g)
Co-Fe_2O_4@PAC	black	micropore	3.31	0.316	595.6

Effect of pH on dye degradation

pH is one of the effective parameters on the dye degradation by nanocomposite. The results of the pH effect on dye removal are presented in Figure 3a. As can be seen, with increasing of pH from 3 to 11, removal efficiency of AO7 dye by H_2O_2/Co-Fe_2O_4@PAC was decreased from 81.5% to 24.5%. According to the results, the removal efficiency of AO7 dye by PMS/Co-Fe_2O_4@PAC increased from 58.5% to 85.4% by increasing pH from 3 to 4; but the increasing of pH up to 4 led to a decrease in the removal efficiency.

The impact of pH also depends on the zeta potential of the catalyst (15,23). For determining pHzpc, 50 mL NaCl 0.01M was added to 10 beakers and pH was adjusted between 2-11 using HCl and NaOH. Then, 0.2 g nanocomposite was added to each beaker and stirred for 48h. The final pH was measured and the initial pH was drawn against the difference of the final pH and the initial pH. pHzpc was obtained from the confluence of the curve with pHzpc zero line that was equal to 6 (Figure 3b).

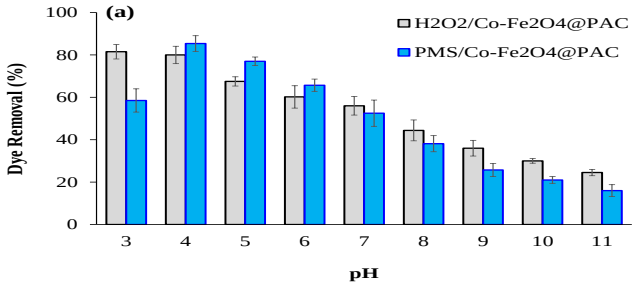

(a)

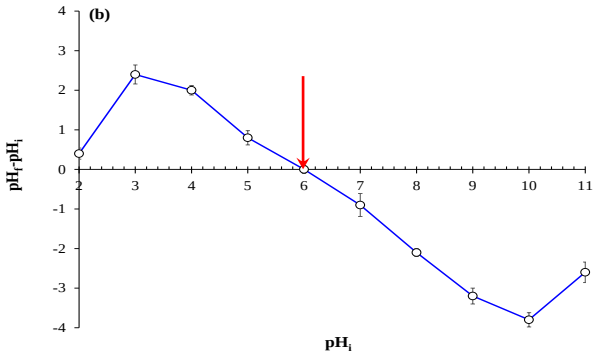

(b)

Figure 3) a) Effect of pH on catalytic degradation of AO7 dye; b) pHzpc (Initial dye concentration: 50 mg/L, H_2O_2 concentration: 10 mM, PMS concentration: 25 µM, Temperature: 298 ºk, Time: 120 min, Catalyst dose: 1 g/L)

Effect of catalyst dosage on dye degradation

One of the effective parameters in the advanced oxidation processes is the catalyst dosage (Figure 4). The removal efficiency of AO7 dye in the presence of H_2O_2 increased from 3% to 78.5 % with increasing the catalyst dose from 0.1 to 1.5 g/L. When PMS was used, the removal efficiency increased from 38.3 % to 86.8 %.

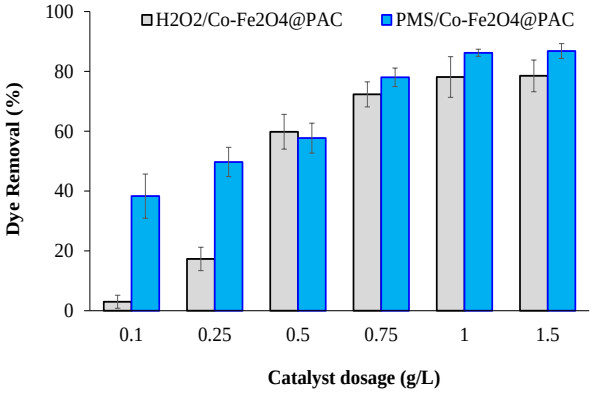

Figure 4) Effect of catalyst dosage on catalytic degradation of AO7 dye (Initial dye concentration: 50 mg/L, H_2O_2 concentration: 10 mM, PMS concentration: 25 µM, Temperature: 298 ºk, Time: 120 min, pH: 4)

Effect of oxidant concentration on dye degradation

The oxidant concentration (in the range of 1-15 mM for H_2O_2 and 2.5-50 µM for PMS) was also investigated. According to results, in the absence of H_2O_2 and PMS, the removal efficiency was 41% and 39.7%, respectively. With increasing the oxidant concentration, the removal efficiency increased. So that, by increasing of H_2O_2 concentration from 1 to 10 mM, the removal efficiency increased from 46.5% to 78.6% (Fig.5a). The dye degradation increased from 44.3% to 86.5% as PMS concentration increased from 2.5 to 25 µM (Fig.5b). With increasing the concentration of oxidants over the optimal amount, dye removal decreased. So that the removal efficiency was 78.5% in the concentration of 15 mM hydrogen peroxide. In the concentration of 50 µM PMS, dye removal was equal to 84.3%.

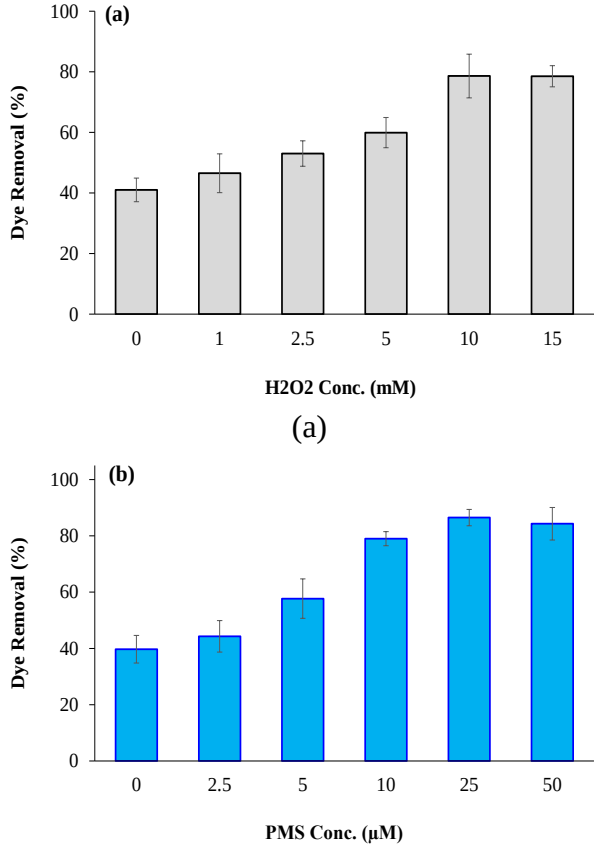

Figure 5) Effect of oxidant concentration [(a)H_2O_2, (b)PMS] on catalytic degradation of AO7 dye (Initial dye concentration: 50 mg/L, Catalyst dose: 1 g/L, Temperature: 298 ºk, Time: 120 min, pH: 4)

Effect of initial dye concentration on dye degradation

The other parameter examined in this study was the effect of initial dye concentration on the rate of decomposition. To survey this parameter, initial concentration between 10-250 mg/L was examined (Figure 6). As can be seen, the maximum degradation rate was achieved at initial concentration of 10 mg/L. The removal efficiency was 99.5% and 99.9% in the presence of H_2O_2 and PMS, respectively. By increasing initial dye concentration to 250 mg/L, the degradation rate decreased (39.7% for H_2O_2 and 43.7% for PMS).

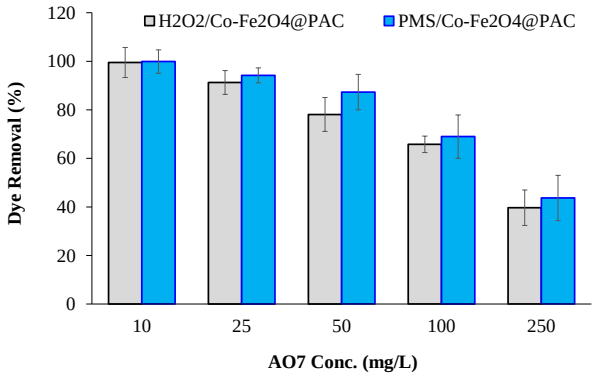

Figure 6) Effect of initial dye concentration on catalytic degradation of AO7 dye (H_2O_2 concentration: 10 mM, PMS concentration: 25 µM, Catalyst dose: 1 g/L, Temperature: 298 K, Time: 120 min, pH: 4)

Effect of reaction time on dye degradation

Effect of reaction time on catalytic degradation of AO7 dye is presented in Figure 7. As the time has increased, the removal efficiency has also increased. With a rise in contact time from 5 to 120 minutes, the removal efficiency in the presence of H_2O_2 and PMS increased from 8.4% to 78.5% and from 9.7% to 87%, respectively. By increasing the reaction time from 60 min to 120 min, no significant change was found in the dye removal efficiency. So that dye removal was 75% and 80.6% in the presence of H_2O_2 and PMS at 60 min, respectively. Thus, optimum reaction time was considered 60 min for next steps of the experiments.

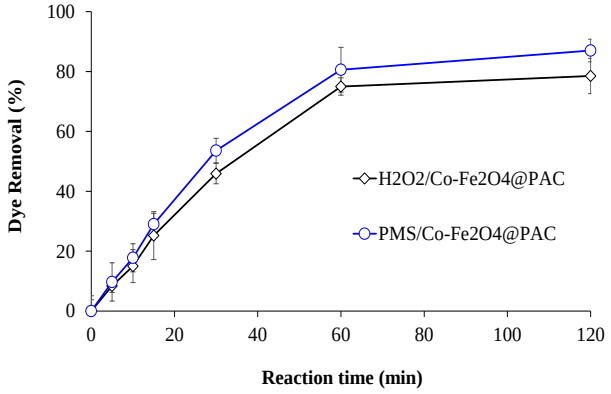

Figure 7) Effect of reaction time on catalytic degradation of AO7 dye

(H_2O_2 concentration: 10 mM, PMS concentration: 25 µM, Catalyst dose: 1 g/L, Temperature: 298 ºk, Initial dye concentration: 50 mg/L, pH: 4)

Kinetic studies

To investigate the AO7 dye absorption behavior by the Co-Fe_2O_4@PAC nanocomposite, kinetic studies were done in the presence of both types of oxidants under optimum conditions. For analyzing experimental data, the first-second-order kinetic model can be used (Eq.3). Figure 8 shows pseudo-first-order kinetic for AO7 dye absorption by nanocomposite.

$$-Ln\frac{C}{C_0} = kt \qquad (3)$$

Where C0 and C are dye concentration at t=0 and t=t (mg/L), respectively. k is the pseudo-first-order rate constant (min^{-1}) and t is reaction time (min) (14).

The kinetic parameters of AO7 dye absorption by the Co-Fe_2O_4@PAC nanocomposite are listed in Table 3. DT90 and t 1/2 are the required time for 90% removal of AO7 dye and half-life, respectively. The results show that the data follow a pseudo-first-order model with the maximum correlation coefficient (R^2>0.99) for both of catalysts.

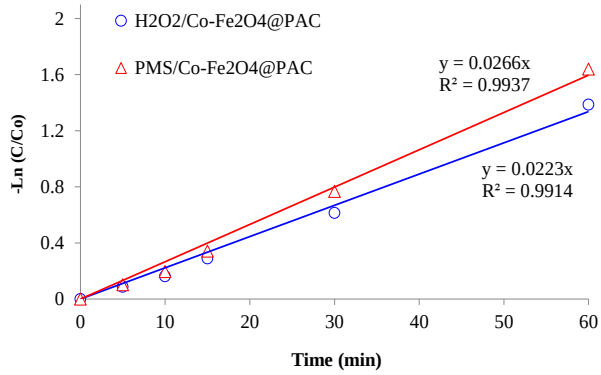

Figure 8) Degradation kinetic of AO7 dye by H_2O_2/Co-Fe_2O_4@PAC and PMS/Co-Fe_2O_4@PAC

Table 3) Kinetic parameters of AO7 dye absorption by the Co-Fe_2O_4@PAC nanocomposite

Nanocomposite	K (min $^{-1}$)	R^2	half-life ($t_{1/2}$ or DT50) (min)	DT90 (min)	
H_2O_2/$CoFe_2O_4$@PAC	0.0223	0.9914	31	103	
PMS/$CoFe_2O_4$@PAC	0.0266	0.9937	26	87	

Comparison of the different processes on degradation of AO7 dye

The degradation of AO7 dye was investigated by different systems under optimum conditions (Figure 9). According to the results, when only H_2O_2 and PMS were added into the solution, very low degradation rate was observed (4.1 % and 7.3%). With the addition of the catalyst (Co-Fe_2O_4@PAC) to solution, a significant improvement was observed in efficiency removal (40.5%). The dye removal in the catalytic system of H_2O_2/Co-Fe_2O_4@PAC was obtained 75.6% and in PMS/Co-Fe_2O_4@PAC system was equal to 81.9%. The results show that peroxymonosulfate has more effect on AO7 dye degradation.

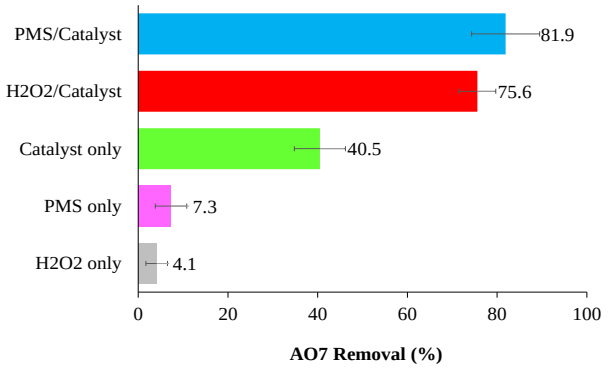

Figure 9) Comparison of the different processes on catalytic degradation of of AO7 dye
(H_2O_2 concentration: 10 mM, PMS concentration: 25 µM, Catalyst dose: 1 g/L, Temperature: 298 ºk, Initial dye concentration: 50 mg/L, pH: 4, Reaction time: 60 min)

Discussion

Effect of pH on dye degradation

The results showed that at pH up to 4, dye removal decreased. At alkaline pH, the surface charge of the catalyst is negative that repulses the anionic dye and reduces dye degradation (23,28). This finding is in concordance with the previous studies. Ahn et al. (2016) investigated PMS activating systems (Pd-Al_2O_3, Co^{2+}, and MWCNTs) for degradation organic pollutants. These researches stated that the reason for the efficiency reduction of 4-CP degradation by nanoparticles at pH 11 is the change of the activator particle surface charge from positive to negative and electrostatic repulsion between nanoparticles and PMS (12).

The pHzpc indicated that at pH<pHzpc the surface of nanocomposite was positively charged and negatively charged at pH>6. In acidic conditions, negatively charged adsorbate by electrostatic attraction leads to the dye adsorption that is negatively charged (23,29).

Effect of catalyst dosage on dye degradation

According to the obtained results, dye removal increased by increasing catalyst dosage. This was attributed to the increase of availability active sites for adsorption and the reaction of AO7 dye with PMS and H_2O_2 (23,30). The obtained results are consistent with the other studies (30,31). Guo et al. (2018) were investigated degradation of Acid Orange 7 by peroxymonosulfate activated with the recyclable nanocomposites of g-C3N4 modified magnetic carbon. Their study results showed that AO7 dye removal increased with the increase of catalyst dosages due to the increased active sites for reaction with PMS (30).

Effect of oxidant concentration on dye degradation

In the present study, the effect of two oxidants (PMS and H_2O_2) on dye degradation were investigated. The results showed that the increasing of oxidant concentration leads to the increase of dye removal. This is due to the more

active radicals produced at higher PMS and H_2O_2 concentrations (30). In the absence of oxidants, the degradation of AO7 dye was very slightly. This is attributed to no production of enough amounts of reactive radical species. At high concentrations, the excessive oxidants act as the radical scavenger. This is due to the combination of the reactive radicals generated at higher concentrations of oxidants (14). The excessive hydrogen peroxide leads to the formation of HO2□ radicals which are weaker radicals relative to hydroxyl radicals and have less activity (32).

Effect of initial dye concentration on dye degradation

The results showed that by increasing the initial dye concentration, dye removal decreased. The reason of the removal efficiency reduction is the decrease of the active sites for the adsorption. With increasing the initial dye concentration, most dye molecules are absorbed on the surface of nanoparticles and prevent the production of hydroxyl radicals (33). In Dargahi et al. (2018) study, the maximum and minimum efficiency was observed at 20 mg/L and 200 mg/L initial dye concentrations, respectively (19).

Effect of reaction time on dye degradation

The obtained results showed that decolorization increases rapidly in the initial stages of reaction time and reach equilibrium at 60 min. The increase of reaction time leads to the high availability to the active sites and produce more hydroxyl radicals. Ahmadi et al. (2018) in their study about the degradation of Reactive Blue 19 dye using H_2O_2/MgO nanoparticles, achieved similar results (15). In another study by Tavassoli et al. (2017), the dye removal by magnetite iron oxide/silica gel nanocomposite was occurred quickly and large amounts of the dye was removed within 40 min and then reach the equilibrium in 50 min (34).

Compare different systems in the dye degradation

The efficiency of different systems (H_2O_2 only, PMS only, catalyst only, H_2O_2/catalyst, and PMS/catalyst) was investigated for the dye degradation. In the presence of H_2O_2,OH radicals are produced that lead to oxidizing the pollutants with high oxidizing capacity (15,35). The results showed that dye removal is much more efficient in the presence of PMS than H_2O_2. Peroxymonosulfate is activated to produce both sulfate and hydroxyl radicals.

Conclusion

In this study, CoFe2O4 nanoparticle was synthesized by co-precipitation method and coated on the modified powdered activated carbon (PAC). The nanocomposite efficiency was investigated for the degradation of AO7 dye. The under optimum conditions (10 mg/L initial dye concentration, 1 g/L nanocomposite dosage, 10 mM H_2O_2, 25 µM PMS after the 120 min at pH 4, the removal efficiency was observed 99.5% and 99.9% in the presence of H_2O_2 and PMS, respectively. According to the obtained results, the removal efficiency of AO7 dye by PMS/Co-Fe_2O_4@PAC system was higher than H_2O_2/Co-Fe_2O_4@PAC system. It can be found that the Co-Fe_2O_4@PAC nanocomposite can be used effectively for the removal of the organic pollutants.

Footnotes

Acknowledgements

The authors wish to acknowledge the members of Environmental Technologies Research Center, Ahvaz Jundishapur University of Medical Sciences, Ahvaz, Iran.

Funding/Support:

The present manuscript was obtained from a research project (project number: 96s68) that financially supported by Ahvaz Jundishapur University of Medical Sciences.

Conflict of Interest:

The authors declared no conflict of interest.

References

1. Ertugay N, Acar FN. The degradation of Direct Blue 71 by sono, photo and sonophotocatalytic oxidation in the presence of ZnO nanocatalyst. Appl Surf Sci 2014;318:121-6. Link

2. Ghaneian M, Jamshidi B, Dehvari M, Amrollahi M. Pomegranate seed powder as a new biosorbent of reactive red 198 dye from aqueous solutions: adsorption equilibrium and kinetic studies. Res Chem Intermed 2015;41(5):3223-34. Link

3. Dehvari M, Ehrampoush MH, Ghaneian MT, Jamshidi B, Tabatabaee M. Adsorption Kinetics and Equilibrium Studies of Reactive Red 198 Dye by Cuttlefish Bone Powder. Iranian J Chem Chem Eng 2017;36(2):143-51. Link

4. Royer B, Cardoso NF, Lima EC, Ruiz VS, Macedo TR, Airoldi C. Organofunctionalized kenyaite for dye removal from aqueous solution. J Colloid Interface Sci 2009;336(2):398-405. PubMed

5. Stoyanova M, Slavova I, Ivanova V. Catalytic performance of supported nanosized cobalt and iron–cobalt mixed oxides on MgO in oxidative degradation of Acid Orange 7 azo dye with peroxymonosulfate. Appl Catal A General. 2014;476:121-32. Link

6. Saggioro EM, Oliveira AS, Pavesi T, Maia CG, Ferreira LFV, Moreira JC. Use of titanium dioxide photocatalysis on the remediation of model textile wastewaters containing azo dyes. Molecules 2011;16(12):10370-86. PubMed

7. Soltani RDC, Khataee A, Safari M, Joo S. Preparation of bio-silica/chitosan nanocomposite for adsorption of a textile dye in aqueous solutions. Int Biodeterior Biodegradation 2013;85:383-91. Link

8. Anipsitakis GP, Dionysiou DD. Radical generation by the interaction of transition metals with common oxidants. Environ Sci Technol 2004;38(13):3705-12. PubMed

9. Lutze H. Sulfate radical based oxidation in water treatment. Universität Duisburg-Essen. 2013.

10. Rodriguez S, Vasquez L, Costa D, Romero A, Santos A. Oxidation of Orange G by persulfate activated by Fe (II), Fe (III) and zero valent iron (ZVI). Chemosphere 2014;101:86-92. Link

11. Xiong X, Sun B, Zhang J, Gao N, Shen J, Li J, et al. Activating persulfate by Fe0 coupling with weak magnetic field: performance and mechanism. Water Res 2014;62:53-62. PubMed

12. Ahn Y-Y, Yun E-T, Seo J-W, Lee C, Kim SH, Kim J-H, et al. Activation of peroxymonosulfate by surface-loaded noble metal nanoparticles for oxidative degradation of organic compounds. Environ Sci Technol 2016;50(18):10187-97. PubMed

13. Jiang J, Zou J, Zhu L, Huang L, Jiang H, Zhang Y. Degradation of methylene blue with H_2O_2 activated by peroxidase-like Fe_3O_4 magnetic nanoparticles. J Nanosci Nanotechnol 2011;11(6):4793-9. PubMed

14. Wang N, Zhu L, Wang M, Wang D, Tang H. Sono-enhanced degradation of dye pollutants with the use of H_2O_2 activated by Fe_3O_4 magnetic nanoparticles as peroxidase mimetic. Ultrason Sonochem 2010;17(1):78-83. PubMed

15. Ahmadi S, Mohammadi L, Igwegbe CA, Rahdar S, Banach AM. Application of response surface methodology in the degradation of Reactive Blue 19 using H_2O_2/MgO nanoparticles advanced oxidation process. Int J Ind Chem 2018;9(3):241-53. Link

16. Qu D, Wang L, Zheng D, Xiao L, Deng B, Qu D. An asymmetric supercapacitor with highly dispersed nano-Bi_2O_3 and active carbon electrodes. J Power Sources 2014;269:129-35. Link

17. Yang N, Zhu S, Zhang D, Xu S. Synthesis and properties of magnetic Fe3O4-activated carbon nanocomposite particles for dye removal. Mater Lett 2008;62(4-5):645-7. Link

18. Zhou L, Ji L, Ma P-C, Shao Y, Zhang H, Gao W, et al. Development of carbon nanotubes/$CoFe_2O_4$ magnetic hybrid material for removal of tetrabromobisphenol A and Pb (II). J Hazard Mater 2014;265:104-14. PubMed

19. Dargahi A, Samaghandi M, Vaziri Y, Ahmadidoost G. Photocatalytic Activity of Zinc Oxide Nanoparticles Coated on Activated Carbon Made from Mango Seed in Removing Acid Black 1 from Aqueous Solutions. Arch Hyg Sci 2018;7(4):242-50. Link

20. Kakavandi B, Rezaei Kalantary R, Jonidi Jafari A, Esrafily A, Gholizadeh A, Azari A. Efficiency of powder activated carbon magnetized by Fe_3O_4 nanoparticles for amoxicillin removal from aqueous solutions: Equilibrium and kinetic studies of adsorption process. Iranian J Health Environ 2014;7(1):21-34. (Full Text Persian) Link

21. Harraz F, Mohamed R, Rashad M, Wang Y, Sigmund W. Magnetic nanocomposite based on titania–silica/cobalt ferrite for photocatalytic degradation of methylene blue dye. Ceram Int 2014;40(1):375-84. Link

22. Ai L, Huang H, Chen Z, Wei X, Jiang J. Activated carbon/CoFe2O4 composites: facile synthesis, magnetic performance and their potential application for the removal of malachite green from water. Chem Eng J 2010;156(2):243-9. Link

23. Santhosh C, Daneshvar E, Kollu P, Peräniemi S, Grace AN, Bhatnagar A. Magnetic SiO_2@ $CoFe_2O_4$ nanoparticles decorated on graphene oxide as efficient adsorbents for the removal of anionic pollutants from water. Chem Eng J 2017;322:472-87. Link

24. Marković D, Šaponjić Z, Radoičić M, Radetić T, Vodnik V, Potkonjak B, et al. Sonophotocatalytic degradation of dye CI Acid Orange 7 by TiO_2 and Ag nanoparticles immobilized on corona pretreated

polypropylene non-woven fabric. Ultrason Sonochem 2015;24:221-9. PubMed
25. Nourmoradi H, Ghiasvand A, Noorimotlagh Z. Removal of methylene blue and acid orange 7 from aqueous solutions by activated carbon coated with zinc oxide (ZnO) nanoparticles: equilibrium, kinetic, and thermodynamic study. Desalination Water Treat 2015;55(1):252-62. Link
26. Wang Y, Sun H, Ang HM, Tadé MO, Wang S. Magnetic Fe_3O_4/carbon sphere/cobalt composites for catalytic oxidation of phenol solutions with sulfate radicals. Chem Eng J 2014;245:1-9. Link
27. Kalam A, Al-Sehemi AG, Assiri M, Du G, Ahmad T, Ahmad I, et al. Modified solvothermal synthesis of cobalt ferrite ($CoFe_2O_4$) magnetic nanoparticles photocatalysts for degradation of methylene blue with H_2O_2/visible light. Results Phys 2018;8:1046-53. Link
28. Zhang T, Zhu H, Croue J-P. Production of sulfate radical from peroxymonosulfate induced by a magnetically separable $CuFe_2O_4$ spinel in water: efficiency, stability, and mechanism. Environ Sci Technol 2013;47(6):2784-91. Link
29. Hassani A, Eghbali P, Metin Ö. Sonocatalytic removal of methylene blue from water solution by cobalt ferrite/mesoporous graphitic carbon nitride ($CoFe_2O_4$/mpg-C3N4) nanocomposites: response surface methodology approach. Environ Sci Pollut Res Int 2018;25(32):32140-55. PubMed
30. Guo F, Lu J, Liu Q, Zhang P, Zhang A, Cai Y, et al. Degradation of Acid Orange 7 by peroxymonosulfate activated with the recyclable nanocomposites of g-C3N4 modified magnetic carbon. Chemosphere 2018;205:297-307. PubMed
31. Yavari S, Mohammad N, Shahmoradi B, Gharibi F, Maleki A. Efficiency of Cobalt Ferrite and Modified Cobalt Ferrite Magnetic Nanoparticles in Removal of Direct Red 23 from Aqueous Solutions: Isotherm and Adsorption Study. J Health 2016;7(3):343-55. (Full Text in Persian) Link
32. Kecić V, Kerkez Đ, Prica M, Lužanin O, Bečelić-Tomin M, Pilipović DT, et al. Optimization of azo printing dye removal with oak leaves-nZVI/H_2O_2 system using statistically designed experiment. J Clean Product 2018;202:65-80. Link
33. Mohaghegh N, Tasviri M, Rahimi E, Gholami MR. Nano sized ZnO composites: Preparation, characterization and application as photocatalysts for degradation of AB92 azo dye. Mater Sci Semicond Process 2014;21:167-79. Link
34. Tavassoli N, Ansari R, Mosayebzadeh Z. Synthesis and Application of Iron Oxide/Silica Gel Nanocomposite for Removal of Sulfur Dyes from Aqueous Solutions. Arch Hyg Sci 2017;6(2):214-20. Link
35. Kaviani D, Asadi M, Khodabakshi MJ, Rezaei Z. Removal of Malachite Green dye from aqueous solution using $MnFe_2O_4$/Al2O3 Nanophotocatalyst by UV/H_2O_2 process. Arch Hyg Sci 2016;5(2):75-84. Link